

Journal of
Applied Remote Sensing

RemoteSensing.SPIEDigitalLibrary.org

Rice yield estimation using Landsat ETM+ Data

Altaf Ali Siyal
Jan Dempewolf
Inbal Becker-Reshef

Rice yield estimation using Landsat ETM+ Data

Altaf Ali Siyal,^{a,b,*} Jan Dempewolf,^c and Inbal Becker-Reshef^c

^aSindh Agriculture University, Faculty of Agricultural Engineering, Tandojam, Pakistan

^bMehran University of Engineering & Technology, U.S.-Pakistan Center for Advanced Studies in Water (USPCAS-W), Jamshoro, Pakistan

^cUniversity of Maryland, Department of Geographical Sciences, 2181 Samuel J. LeFrak Hall, 7251 Preinkert Drive, College Park, Maryland 20742, United States

Abstract. Paddy rice areas in Larkana district in Sindh province, Pakistan, were mapped over eight years. Landsat 7 ETM+ satellite imagery was classified for rice areas using training data collected through visual interpretation and using a bagged decision tree approach. Within the rice areas, we estimated yield for the 2013 season using regression models based on Landsat-derived normalized difference vegetation index (NDVI) and ratio vegetation index (RVI) values against historic, reported yield values. The annual cropped rice area estimated from satellite imagery was between 19% and 24% lower than the area reported by the Crop Reporting Service, Sindh. A positive and strong relationship with coefficient of determination (R^2) of 0.94 was observed between the reported rice crop yield and NDVI at the peak of the growing season for the years 2006 to 2013. A fair relation ($R^2 = 0.875$) between rice crop yield and RVI was observed for the same years. A strong relationship between observed and predicted rice production with model efficiency = 0.925, mean bias error = $-85,016 t$, and RMSE = $80,726 t$ was obtained. Thus, Landsat ETM+ has a high potential for estimating rice yield and production at the district level in Pakistan and elsewhere. © 2015 Society of Photo-Optical Instrumentation Engineers (SPIE) [DOI: [10.1117/1.JRS.9.095986](https://doi.org/10.1117/1.JRS.9.095986)]

Keywords: rice; normalized difference vegetation index; crop yield; remote sensing; Landsat; Pakistan.

Paper 15375 received May 28, 2015; accepted for publication Oct. 19, 2015; published online Nov. 18, 2015.

1 Introduction

Rice, a major food and cash crop, is cultivated in many countries throughout the world. It is reported that paddy rice is cultivated on about 15% of the world's total arable land,^{1,2} with an annual paddy production of about 729 million tons during 2012.³ More than three billion people in the world use rice as their primary food source.⁴ In Pakistan, lowland (paddy) rice is cultivated on an area of over 2.57 million ha,^{5,6} which is 10.9% of the total cultivated area, with an annual production of 9.4 million tons paddy rice or 6.3 tons milled rice during 2012 to 2013⁷ and 5.54 tons during 2013 to 2014.⁶ Pakistan occupies the 13th position in terms of rice production worldwide, and it ranks 4th in rice export. Sindh province of Pakistan contributes approximately 25% to the total national rice production. Larkana is one of the main rice-cultivating districts of Sindh province, producing approximately 20% of the total rice production of the province.

The spatial distribution of paddy fields, monitoring crop development and growth, and the early prediction of crop yield are of great importance for planners and policy makers and for the management of food security and water resources.^{8,9} Timely, accurate, and reliable information can assist planners and decision makers in dealing with deficits or surpluses of crop production. In Pakistan, cultivated area and crop production estimates are usually forecast using field data collected on the ground within a village list frame sampling scheme (Pakistan Bureau of Statistics). However, these reports are often subjective, expensive, laborious, time-consuming, and prone to errors, which may result in poor crop area and yield estimations.¹⁰ Also, in most

*Address all correspondence to: Altaf Ali Siyal, E-mail: siyal@yahoo.com

countries, data on crop area and yield arrive late to analyze, make inferences, and take appropriate measures for avoiding food shortages.¹¹ Remote sensing tools are used worldwide for identification and monitoring of agricultural crops and for forecasting of crop yields and acreage under cultivation.^{12,13}

Different approaches are used to predict crop yields from remotely sensed data. The most common approach is to develop a regression model based on the direct empirical relationship between normalized difference vegetation index (NDVI) measurements and crop yield.^{14–18} This idea assumes that crop yield is directly related to spectral-vegetation indices reflecting photosynthetic capacity of plants and crop vigor, which is affected by a number of factors including fertilizer, water, and pesticides.^{19,20} The correlation between the spectral reflectance of crops and crop yield is widely accepted and used for crop yield predictions.^{15,21} However, it is still not widely integrated into operational monitoring systems.

In order to assess the reliability and accuracy of remote sensing tools, the utility of Landsat 7 ETM+ imagery for mapping rice areas and estimating paddy rice yield for Larkana district located in the southern Sindh province of Pakistan was tested in the present study. The objective of this study was to classify and calculate the area under paddy rice cultivation in Larkana district, a district of southern Sindh province of Pakistan, using Landsat ETM+ images and to assess the feasibility of developing a crop yield model from rice crop yield and the NDVI.

2 Materials and Methods

2.1 Study Area

Larkana is a major rice-growing district in the southern Sindh province of Pakistan and was therefore selected for the study. It is located at 68°7' E to 68°30' E and 27°6' N to 27°58' N, with a mean elevation of 49 ± 4 m above mean sea level, as shown in Fig. 1. The average maximum and minimum temperatures are 42°C and 31°C, respectively, during the summer (Kharif) period from June to September and 21°C and 11°C during the winter (rabi) period from November to March. The annual precipitation in the district is approximately 130 mm, which is insufficient to meet crop water requirements. Thus, agricultural activities depend mainly on two main irrigation

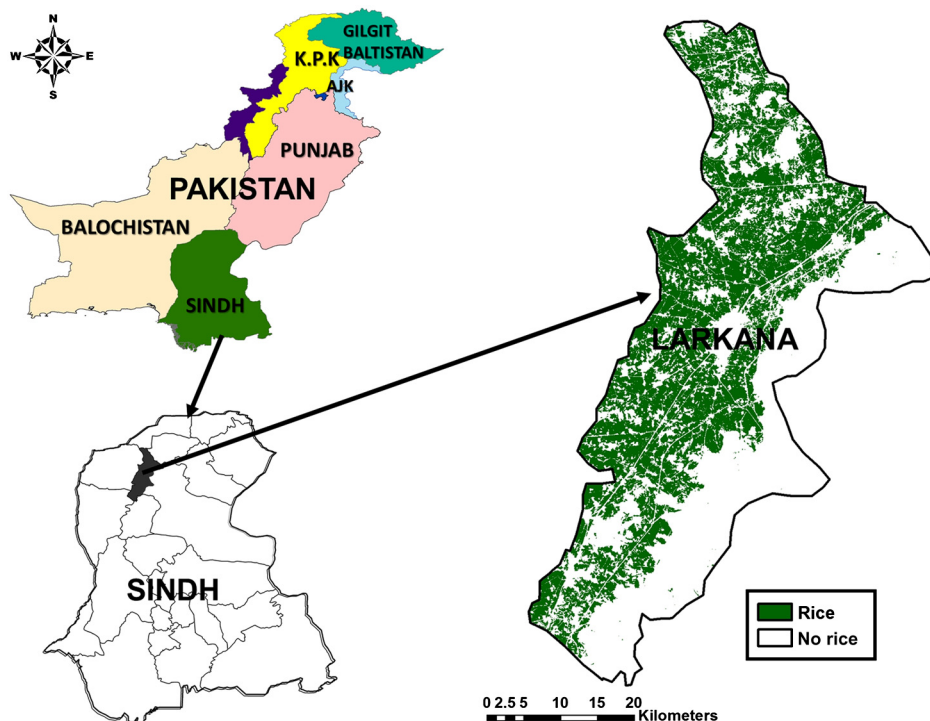


Fig. 1 Location of the study area and the crop mask for the year 2010.

canals, the Rice canal and the Dadu canal, which pass through the district. Rice and wheat crop rotation is common here. During the Kharif season, paddy rice is sown on more than 80% of the agricultural lands, whereas wheat is a dominant crop during the rabi season on approximately 30% of the area. Rice paddy plantation starts every year after mid-June and continues until mid-August. Rice harvesting starts in the middle of October and continues until the end of November.

2.2 Conventional Crop Reporting

In Sindh, the southern province of Pakistan, the first and second crop area estimates are based on sample surveys undertaken by the statistical staff of the Provincial Crop Reporting Services (CRS), Agriculture Department, in the months of July and September for Kharif crops and in December and February for rabi crops. The final crop area estimates are based on a complete enumeration (Girdawari) of all areas carried out by Patwaris (a revenue collector and small administrative unit of the Revenue Department) twice per year. The consolidated information is examined by a subcommittee comprised representatives of the Provincial Revenue, Agriculture, Irrigation, and Bureau of Statistics Departments. Final estimates are approved by the Provincial Agriculture Statistics Coordination Board and estimates are made public. Preliminary estimates of production for all major crops are based on the subjective judgment of the CRS staff. For final estimates, crop-cutting surveys are conducted for wheat, cotton, and rice. Production estimates for remaining major crops are based on subjective judgment and an opinion survey conducted by the CRS. For final estimates, crop-cutting surveys of selected fields (about 100 samples per district) are conducted for all major crops, i.e., wheat, cotton, and rice, by the CRS. The final estimates are checked by a subcommittee comprised of representatives from the Provincial Department of Agriculture, Revenue, Irrigation, and Planning and Development, and after approval from the Provincial Agriculture Statistics Coordination Board, the figures are made public 2 to 6 months after crop harvest. Thus, remote sensing-based early estimates of potential increase or decrease in crop yields help policy and decision makers to allow for timely import or export of agricultural products in the country.

For this study, we obtained the historical data of the area under paddy cultivation, rice yield, and total production for Larkana district over eight years, 2006 to 2013, from the Sindh CRS, Department of Agriculture.

2.3 Landsat

Landsat imagery is an invaluable resource for monitoring global surface change^{22–24} and is a main source of medium spatial resolution earth observations used in decision making. In the present study, we used Landsat ETM+ imagery (WRS-2 path 152, row 41, processing level 1T) from 2006 to 2013. For each year, three images, one after sowing (last week of July), one at the seasonal peak (last week of September), and one after harvest (last week of November) were downloaded from the United States Geological Survey portal at Ref. 25. The total number of Landsat images used in the study were 24 scenes for 8 years from 2006 to 2013 (Table 1). Quick looks are available at GLOVIS.²⁵ The digital numbers (DN) of the Landsat reflective bands were converted to top-of-atmosphere (ToA) reflectance using the standard approach described by Chander et al.²⁶ The images were compared carefully with each other using visual interpretation by overlaying bands from different dates and quickly changing back and forth. No significant deviations of pixel locations or more than one pixel were noticed. This was deemed sufficient for between-image comparisons. Similarly, the geolocation accuracy of the Landsat image to higher-resolution imagery on Google Earth was assessed visually by digitizing landmarks, such as road crossings and buildings on Google Earth, and overlaying them on the Landsat scenes. Similarly, no significant deviations exceeding approximately one pixel were noticed.

2.4 Classification of Rice/Nonrice Areas

Rice crop masks were prepared for each year using three Landsat scenes of the same year from the early growing season, the height of growing season, and after harvest. The classification for

Table 1 Landsat ETM+ images used in the study and their radiometric coefficients.

| S. No | Acquisition date | Path | Row | DOY | d | LMAX | | LMIN | | θ_s |
|-------|---------------------------------|------|-----|-----|---------|--------|--------|-------|-------|------------|
| | | | | | | B3 | B4 | B3 | B4 | |
| 1 | July 15, 2006 ^a | 152 | 41 | 196 | 1.01646 | 234.40 | 241.10 | -5.00 | -5.10 | 64.960952 |
| 2 | October 3, 2006 ^a | 152 | 41 | 276 | 1.00062 | 234.40 | 241.10 | -5.00 | -5.10 | 51.716023 |
| 3 | November 20, 2006 ^a | 152 | 41 | 324 | 0.98624 | 234.40 | 157.40 | -5.00 | -5.10 | 38.417729 |
| 4 | July 18, 2007 ^a | 152 | 41 | 199 | 1.01629 | 234.40 | 241.10 | -5.00 | -5.10 | 64.813437 |
| 5 | September 20, 2007 ^a | 152 | 41 | 263 | 1.00430 | 234.40 | 241.10 | -5.00 | -5.10 | 55.269170 |
| 6 | November 23, 2007 ^a | 152 | 41 | 327 | 0.98750 | 234.40 | 241.10 | -5.00 | -5.10 | 37.813126 |
| 7 | July 20, 2008 ^a | 152 | 41 | 202 | 1.01609 | 234.40 | 241.10 | -5.00 | -5.10 | 64.418581 |
| 8 | September 22, 2008 ^a | 152 | 41 | 266 | 1.00346 | 234.40 | 241.10 | -5.00 | -5.10 | 54.414408 |
| 9 | November 25, 2008 ^a | 152 | 41 | 329 | 0.98712 | 234.40 | 157.40 | -5.00 | -5.10 | 37.153097 |
| 10 | July 23, 2009 ^a | 152 | 41 | 204 | 1.01592 | 234.40 | 157.40 | -5.00 | -5.10 | 64.510850 |
| 11 | September 25, 2009 ^a | 152 | 41 | 268 | 1.00290 | 234.40 | 241.10 | -5.00 | -5.10 | 54.005037 |
| 12 | November 19, 2009 ^b | 152 | 41 | 324 | 0.98809 | 264.00 | 221.00 | -1.17 | -1.51 | 38.476432 |
| 13 | July 10, 2010 ^a | 152 | 41 | 191 | 1.01664 | 234.40 | 241.10 | -5.00 | -5.10 | 65.954912 |
| 14 | September 28, 2010 ^a | 152 | 41 | 271 | 1.00205 | 234.40 | 241.10 | -5.00 | -5.10 | 53.580597 |
| 15 | November 23, 2010 ^b | 152 | 41 | 327 | 0.98750 | 264.00 | 221.00 | -1.17 | -1.51 | 37.801484 |
| 16 | July 13, 2011 ^a | 152 | 41 | 194 | 1.01655 | 234.40 | 241.10 | -5.00 | -5.10 | 66.044381 |
| 17 | October 1, 2011 ^a | 152 | 41 | 274 | 1.00119 | 234.40 | 241.10 | -5.00 | -5.10 | 52.959430 |
| 18 | November 18, 2011 ^a | 152 | 41 | 322 | 0.98851 | 234.40 | 157.40 | -5.00 | -5.10 | 39.371435 |
| 19 | July 31, 2012 ^a | 152 | 41 | 213 | 1.01497 | 234.40 | 241.10 | -5.00 | -5.10 | 64.807901 |
| 20 | October 3, 2012 ^a | 152 | 41 | 277 | 1.00033 | 234.40 | 241.10 | -5.00 | -5.10 | 52.513214 |
| 21 | November 20, 2012 ^a | 152 | 41 | 325 | 0.98789 | 234.40 | 157.40 | -5.00 | -5.10 | 38.943448 |
| 22 | July 18, 2013 ^a | 152 | 41 | 199 | 1.01629 | 234.40 | 241.10 | -5.00 | -5.10 | 66.038216 |
| 23 | September 20, 2013 ^a | 152 | 41 | 263 | 1.00430 | 234.40 | 241.10 | -5.00 | -5.10 | 56.168672 |
| 24 | November 7, 2013 ^a | 152 | 41 | 311 | 0.99102 | 234.40 | 241.10 | -5.00 | -5.10 | 42.320757 |

^aLandsat 7.^bLandsat 5.

rice versus nonrice areas involved the following three steps and was carried out separately for each year.

1. The Landsat bands 3, 4, 5, 6, and 7 of all three scenes were stacked on top of each other and saved into a single 15-band image file.
2. Training areas for rice fields were identified using visual interpretation of the multi-temporal Landsat imagery in combination with very high-resolution imagery from Google Earth and, crucially, applying the local expert knowledge of the analyst, who is producing rice himself in the study area and is very familiar with it. Emphasis was placed on the edges of rice fields, selecting training areas of rice, and nonrice along the field boundaries. In addition, small samples of nonrice training

areas of land cover types, which did not occur in the immediate vicinity of rice fields, were digitized across the area.

3. The classification was carried out using a bagged decision tree approach.²⁷ A decision tree is a nonparametric, binary classifier. It is constructed by repeatedly splitting the training data based on Landsat band values so that the homogeneity of the land cover classes of the two new subsets resulting from each binary split is maximized. The construction of only one decision tree can lead to overfitting of the classification model, reducing the accuracy of the result when applying the decision tree to the entire study area. This can be improved by calculating several decision trees, in our case a total of seven trees, and excluding from each tree 20% of the training data selected at random with replacement.^{28,29} For the final result, all seven trees are applied to the entire study area, and for each pixel a majority vote is carried out, i.e., if four of the decision trees indicate rice and three indicate nonrice, then the rice class is assigned as the final classification result.

Using this methodology, rice crop masks of the scenes for all eight years were prepared and subset to Larkana district (Fig. 2) and the area under rice crop for each year was calculated.

2.5 Calculation of Missing Data in Landsat 7 Images

The scan line corrector (SLC) in the ETM+ instrument of Landsat 7 stopped functioning on May 31, 2003, which resulted in double imaging of some areas, whereas others were not imaged at all. The net effect of Landsat ETM+ SLC being off is missing data of approximately 22% for the normal entire scene area.^{30,31} However, the stripes of missing data for the area under study (Larkana district) amount to between 3% (5723 ha) and 5% (9540 ha). The total area is small because the study area falls close to the center of the swath (nadir) where the missing-data stripes converge, and the amount of missing data is significantly less than the average for the entire scene [Fig. 2(a)]. Rice area for the missing data pixels was estimated by calculating the ratio of rice versus nonrice for the area for which Landsat data existed and applying the same ratio to the areas of missing data.

2.6 Data Analysis

2.6.1 Conversion of Landsat Digital Numbers to Top-of-Atmosphere Reflectance

For all Landsat bands, the DN were first converted to radiance and then to ToA reflectance using Eqs. (1) and (2) as described by Chander et al.²⁶ The radiometric coefficients used in this study are given in Table 1,

$$L_{\lambda} = \left(\frac{LMAX_{\lambda} - LMIN_{\lambda}}{Q_{calmax} - Q_{calmin}} \right) (Q_{calmax} - Q_{calmin}) + LMIN_{\lambda}, \quad (1)$$

$$\rho_{\lambda} = \frac{\pi L_{\lambda} d^2}{ESUN_{\lambda} \cos \theta_s}, \quad (2)$$

where L_{λ} is the spectral radiance at the sensor's aperture [$W/(m^2 sr \mu m)$], $LMIN_{\lambda}$ is the spectral at-sensor radiance scaled to Q_{calmin} [$W/(m^2 sr \mu m)$], $LMAX_{\lambda}$ is the spectral at-sensor radiance scaled to Q_{calmax} [$W/(m^2 sr \mu m)$], Q_{cal} is the quantized calibrated pixel value (DN), Q_{calmin} is the minimum quantized calibrated pixel value corresponding to $LMIN_{\lambda}$ (DN). It is always 1, Q_{calmax} = maximum quantized calibrated pixel value corresponding to $LMAX_{\lambda}$ (DN). It is always 255, ρ_{λ} is the planetary TOA reflectance, π is the mathematical constant pi, d is the earth-sun distance [astronomical units], $ESUN_{\lambda}$ is the mean exoatmospheric solar irradiance. For band 3 (red), it is 1536 [$W/(m^2 sr \mu m)$], and for band 4, (NIR) it is 1145 [$W/(m^2 \mu m)$], and θ_s is the sun elevation (deg).

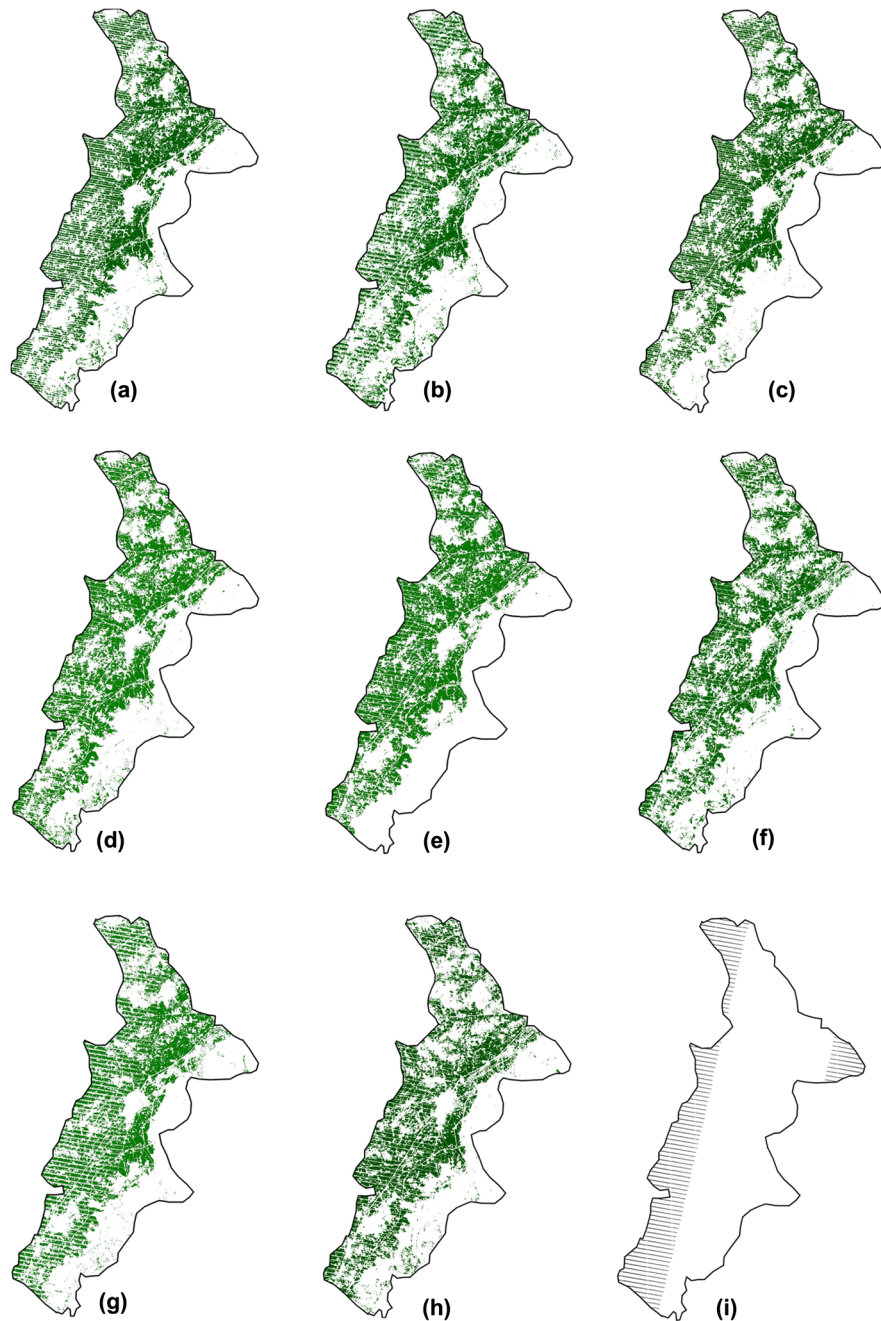


Fig. 2 Rice crop masks of Larkana district from 2006 to 2013. Crop mask for the years: (a) 2006, (b) 2007, (c) 2008, (d) 2009, (e) 2010, (f) 2011, (g) 2012, (h) 2013, and (i) no data mask.

No atmospheric correction of the acquired satellite imagery was carried out because it is unnecessary for the image classification method that we used in the present study.

2.7 Calculation of Vegetation Indices

The NDVI is sensitive to green vegetation vigor. It is calculated from the visible and near-infrared light reflected by the target surface. The RVI is a commonly used vegetation index calculated as the near-infrared reflectance divided by the visible red reflectance values. Landsat bands 3 and 4 converted to ToA were used to calculate the two vegetation indices, NDVI,³² and ratio vegetation index (RVI),³³ as described in Eqs. (3) and (4). The indices were calculated for the Landsat

scenes at the peak of each growing season at the end of September/beginning of October for all pixels under rice cultivation

$$\text{NDVI} = \frac{\rho_{\text{nir}} - \rho_{\text{red}}}{\rho_{\text{nir}} + \rho_{\text{red}}}, \quad (3)$$

$$\text{RVI} = \frac{\rho_{\text{nir}}}{\rho_{\text{red}}}, \quad (4)$$

where ρ_{nir} is the near-infrared reflectance and ρ_{red} is the red reflectance.

The NDVI and RVI for rice crop in Larkana district from 2006 to 2013 were computed and are summarized in Table 3.

2.8 Development of the Rice Yield Model

We calculated a linear regression model based on the relationship between the rice crop yield of Larkana district (reported by CRS, Sindh) from 2006 to 2013 and the respective NDVI and RVI peak of the same season, approximately 60 to 70 days after sowing of crops (see Fig. 3 for time of peak NDVI). We used NDVI 60 to 70 days after rice transplanting because this is the peak of the rice-growing season.

We estimated the crop yield (tons/ha) for each year from NDVI using regression by adopting the following method: for each year, we calculated a regression equation between CRS-reported yield and NDVI (excluding the year to be predicted), then applied the regression equation to that year. For example, for the year 2009, we used NDVI and CRS yield values from 2006, 2007, 2008, 2010, 2011, 2012, and 2013 to calculate the regression equation and applied it to the year 2009. Similarly, for the year 2011 yield estimation, the data values from 2006, 2007, 2008, 2009, 2010, 2012, and 2013 were used, and so on.

2.9 Accuracy Assessment of Rice Yield Model

The agreement between the total rice production of the district reported by CRS and the rice production estimated from the rice yield prediction model (based on the peak NDVI and RVI of the crop), multiplied by the area estimated from remote sensing, was quantified in terms of three statistical indicators: the mean bias error (MBE), root mean square error (RMSE), and model efficiency (ME). The magnitude of bias was considered a better indicator of model performance in the comparisons. These parameters are defined as follows.³⁵

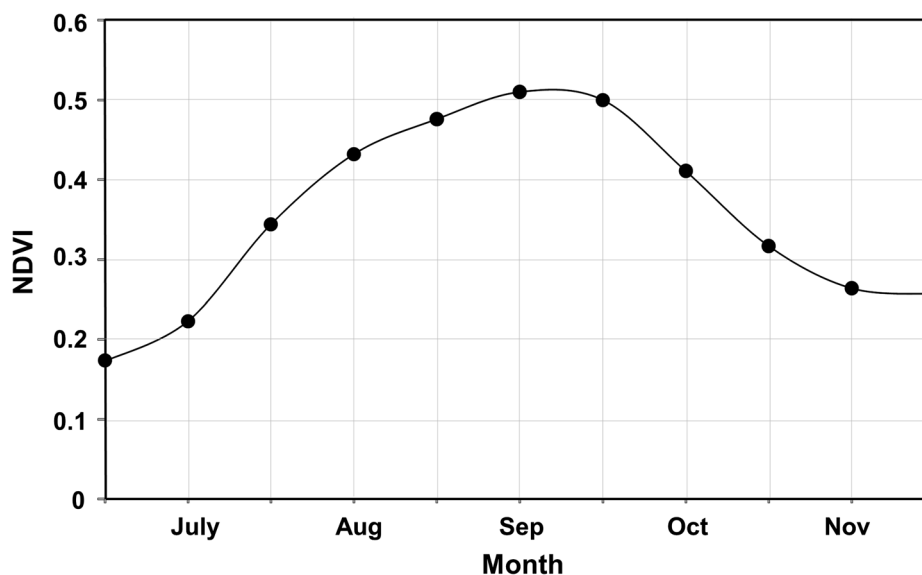


Fig. 3 Mean normalized difference vegetation index (NDVI) (based on MODIS data) of Larkana district from 2000 to 2014 [Source: GLAM Pakistan³⁴].

2.9.1 Mean bias error

An MBE indicates the potential bias (i.e., underestimation and overestimation) in the predicted yield values. A low MBE is usually desired for a model. A positive MBE gives the average amount of overestimation in the calculated value and vice versa. Mathematically,³⁶

$$\text{MBE} = \frac{\sum_{i=1}^n (P_i - O_i)}{n}, \quad (5)$$

where n is the number of data points, P_i is the i 'th model predicted data point, O_i is the i 'th observed data, and \bar{O} is the mean of observed data.

2.9.2 Root mean square error

RMSE is a frequently used measure of the differences between values predicted by a model and the values actually observed/measured. The RMSE is always positive; a zero value is considered ideal

$$\text{RMSE} = \sqrt{\frac{\sum_{i=1}^n (P_i - O_i)^2}{n}}. \quad (6)$$

2.9.3 Model efficiency

An ME coefficient is used to evaluate the prediction potential of a model. An ME of 1 is a perfect match of modeled data to the observed data. An efficiency of 0 shows that the model predictions are as accurate as the mean of the observed data, whereas an efficiency less than zero occurs when the observed mean is a better predictor than the model. Essentially, the closer the ME is to 1, the more accurate the model is³⁶

$$\text{ME} = \frac{[\sum_{i=1}^n (O_i - \bar{O})^2 - \sum_{i=1}^n (P_i - O_i)^2]}{[\sum_{i=1}^n (O_i - \bar{O})^2]}. \quad (7)$$

3 Results

3.1 Estimation of Area Under Rice Cultivation

The area under rice cultivation in Larkana district from 2006 to 2013 reported by CRS and the area calculated from the classified satellite imagery is plotted in Fig. 4. It shows that the reported rice acreage ranged between 84,100 ha in 2010 and 98,009 ha in 2013, whereas area determined from the classified imagery ranged from 70,819 to 75,580 ha in 2010 and 2009, respectively. Thus, the rice-crop area determined from the classified maps is between 19% and 24% lower than the reported area by CRS. Wardlow and Egbert³⁷ reported that the classified cropped areas based on MODIS satellite data were within 1% to 5% of USDA-reported crop areas for most classes at the state level. Reasons for this discrepancy can be manifold. First of all, field-based methods applied by crop reporters are based on field size. However, they do not account for variability within each field. In some cases, the rice crop will have only emerged in one part of the field, or it can be severely damaged by pest or disease. The satellite imagery will respond to the changed surface reflectance with a reduction in the estimated area of rice, whereas the field-based method based on field sizes does not. A second important reason is the resolution of the satellite imagery. Edge pixels at 30-m resolution are not included in the rice area estimate, because these pixels are not pure and including them in the training as rice would result in a large number of misclassified pixels. A solution to this problem would be the use of much higher resolution satellite imagery such as RapidEye (5 m) or Worldview-2 (1.84-m multispectral). This kind of imagery, however, is not free and was not available for this study. A

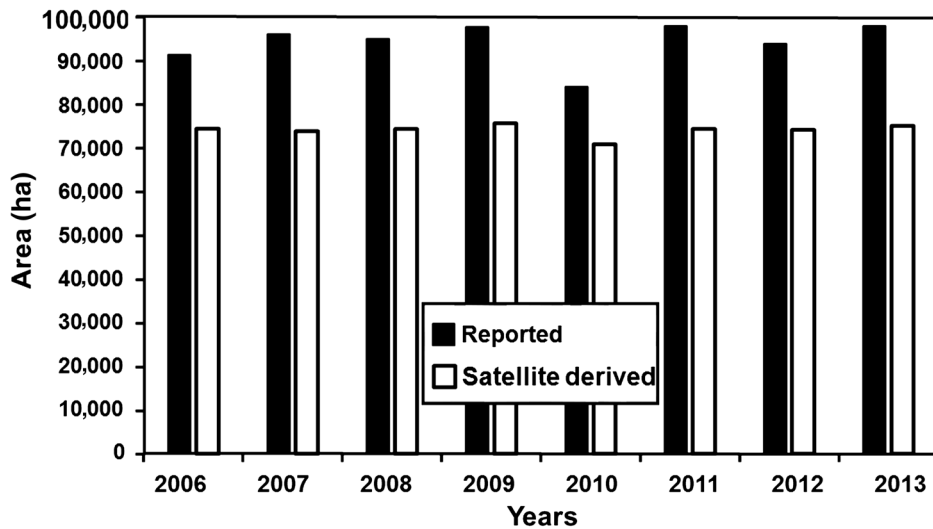


Fig. 4 Area under rice cultivation in Larkana district from 2006 to 2013.

third reason is that CRS relies on farmer surveys for the area estimates instead of actual measurements, which introduces an additional source of error.

The rice acreage in Larkana district reported by CRS is plotted against acreage calculated from crop masks in Fig. 5.

A moderate linear regression equation with goodness of fit $R^2 = 0.827$ based on the classified and reported acreage was developed and is given below:

$$C_a = 2.982 \times \text{CRS}_a - 126,488, \quad (8)$$

where C_a and CRS_a are the rice acreage determined from the crop masks and reported by CRS, respectively.

The scattering of data points in Fig. 5 can be categorized into a single point (down left) and a points cluster (up right). The single point (outlier) might have increased the goodness of fit

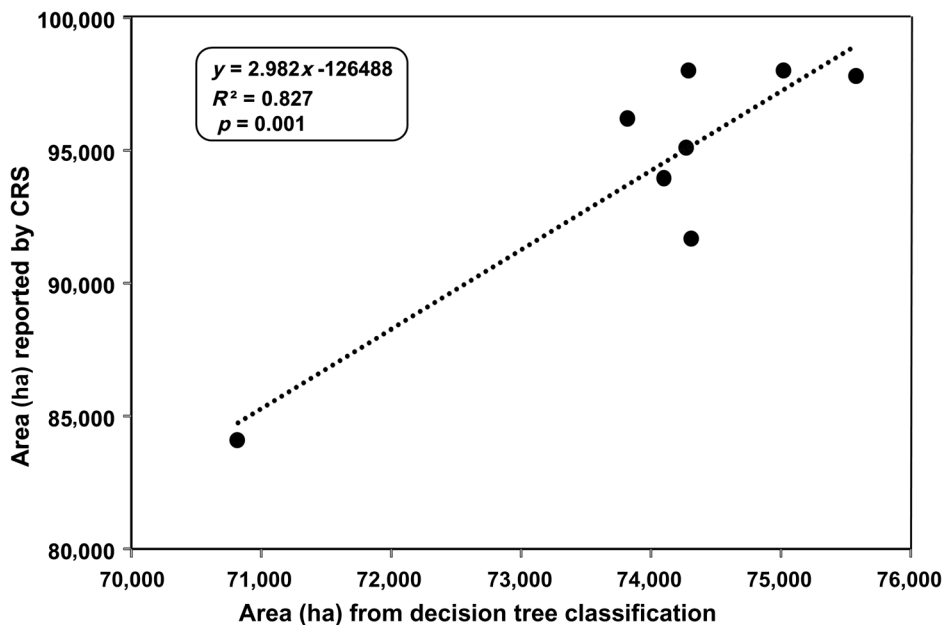


Fig. 5 Relation between the acreage under rice in Larkana district reported by CRS and determined by classified maps from 2006 to 2013.

($R^2 = 0.83$). To analyse the effect of the single point (outlier) on goodness of fit, it was removed from the data. As a result, the R^2 value decreased to 0.72, but it did not affect the p value. Hence, the correlation was still positive and within a reasonable range.

3.2 Crop Yield and Total Production

The yearwise total rice production and yield of all districts of Sindh are usually published 4 to 6 months after harvest by the Department of Agriculture, Government of Sindh, Pakistan, and are given in Table 2.

The estimated crop yield (tons/ha) of considered years was multiplied by the respective rice-cropped area obtained from the satellite imagery to estimate total rice production of the district. Figure 6 shows the total rice production (tons) reported by CRS and calculated after multiplying

Table 2 Year-wise rice-cropped area, yield, and total production reported by CRS as well as cropped area and total production estimated from the Landsat imagery.

| Year | Reported by CRS | | | From satellite imagery | | |
|------|-----------------|-------------------------|-----------------|------------------------|---------------------------|-----------------------------------|
| | Area (hac) | Total Production (Tons) | Yield (Tons/ha) | Estimated Area (hac) | Estimated Yield (Tons/ha) | Estimated total Production (Tons) |
| 2006 | 91,500 | 283,400 | 3.097 | 74,352 | 3.166 | 235,399 |
| 2007 | 96,200 | 327,900 | 3.409 | 73,820 | 3.356 | 247,740 |
| 2008 | 95,100 | 370,200 | 3.893 | 74,273 | 3.980 | 295,607 |
| 2009 | 97,800 | 383,600 | 3.922 | 75,580 | 3.826 | 289,169 |
| 2010 | 84,100 | 328,700 | 3.908 | 70,819 | 3.774 | 267,271 |
| 2011 | 98,000 | 388,400 | 3.963 | 74,289 | 4.137 | 307,334 |
| 2012 | 93,950 | 362,100 | 3.854 | 74,101 | 3.784 | 280,400 |
| 2013 | 98,009 | 322,400 | 3.289 | 75,020 | 3.394 | 254,617 |

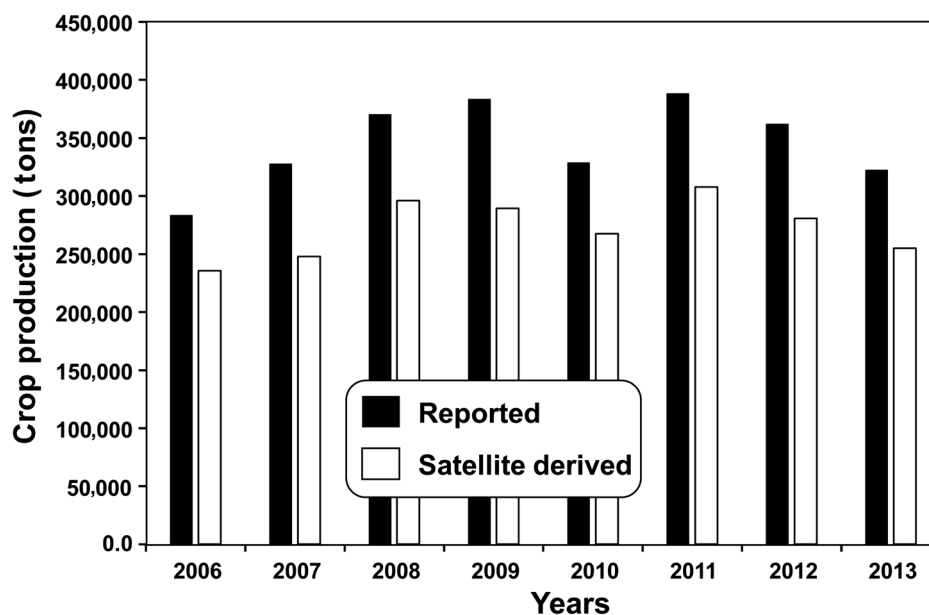


Fig. 6 Rice crop production (in metric tons) of Larkana district from 2006 to 2013 reported by CRS and calculated from satellite classified map.

the estimated yield with area determined from imagery after classification. The figure shows that the total rice production of the district from 2006 to 2013 based on area determined from the satellite imagery is 17% to 24% lower than that reported by CRS. This is because the cropped area reported by CRS is 19% to 24% higher than that obtained from satellite imagery. Hence, the total rice production of the district calculated using the classified area is 17% to 24% lower than that reported by CRS. This might be due to the fact that the two area estimates are derived using entirely different methods and to a degree measure two different parameters. The field surveys are based on area sown and use the entire area of agricultural fields, sometimes obtained through farmer surveys rather than measurements. Thus, such surveys are said to be poor predictors in Pakistan, where spatial variability in soil and water management practices are present. The satellite, on the other hand, sees only the areas actually covered by crop and excludes areas within fields that did not germinate or were damaged. Furthermore, the satellite analysis uses pure pixels and disregards mixed pixels at the edges of agricultural fields, introducing a potential bias toward reduced crop area.

3.3 Relationship Between Vegetation Indices and Rice Yield

The NDVI and RVI vegetation indices based on the average maximum NDVI value over all rice area in the study area for the years 2006 to 2013 computed from Landsat imagery of the Larkana district and acquired 60 to 70 days after rice sowing are given in Table 3.

From the mathematical point of view, both indices are functionally equivalent and contain the same information.³⁸ Thus, NDVI has a similar trend to that of RVI. It can be concluded that the NDVI and RVI indices can be effective tools for monitoring the rice-cultivated area, as also reported by Oguro et al.³⁹

Figure 7 shows the linear relationship between average peak NDVI and rice crop yield (2006 to 2013) reported by CRS. The plot shows a positive relationship of NDVI with crop yield of the district. A strong relationship with a coefficient of determination (R^2) of 0.94 was observed between rice crop yield (2006 to 2013) and average peak NDVI of the respective years calculated from Landsat imagery. The following relation between NDVI and rice crop yield was obtained

$$\text{Crop yield} = 23.641 \text{ NDVI} - 10.343. \quad (9)$$

A fair relation ($R^2 = 0.875$) between rice crop yield reported by CRS and average RVI computed from the temporal imagery of Larkana district was observed (Fig. 8), with the statistical relation as:

Table 3 Average NDVI and RVI of rice crop from 2006 to 2013 grown in Larkana district, Sindh, Pakistan.

| S. No. | Year | NDVI | RVI |
|--------|------|-------|------|
| 1 | 2006 | 0.570 | 3.75 |
| 2 | 2007 | 0.580 | 4.05 |
| 3 | 2008 | 0.605 | 5.11 |
| 4 | 2009 | 0.600 | 5.10 |
| 5 | 2010 | 0.590 | 4.50 |
| 6 | 2011 | 0.610 | 6.10 |
| 7 | 2012 | 0.598 | 4.92 |
| 8 | 2013 | 0.580 | 4.00 |

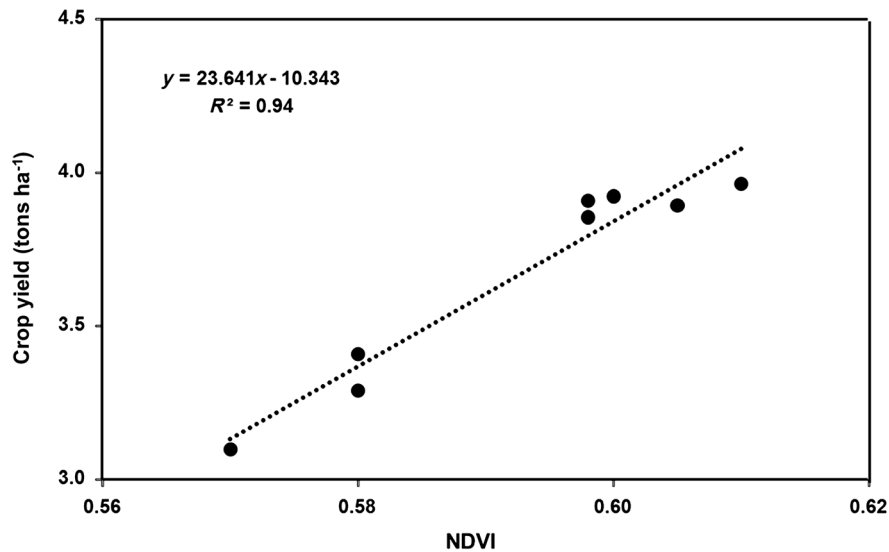


Fig. 7 Relationship between the average NDVI of the rice crop in Larkana district and the average crop yield from 2006 to 2013. NDVI is determined from imagery of the area captured after 60 to 70 days from the sowing of crops.

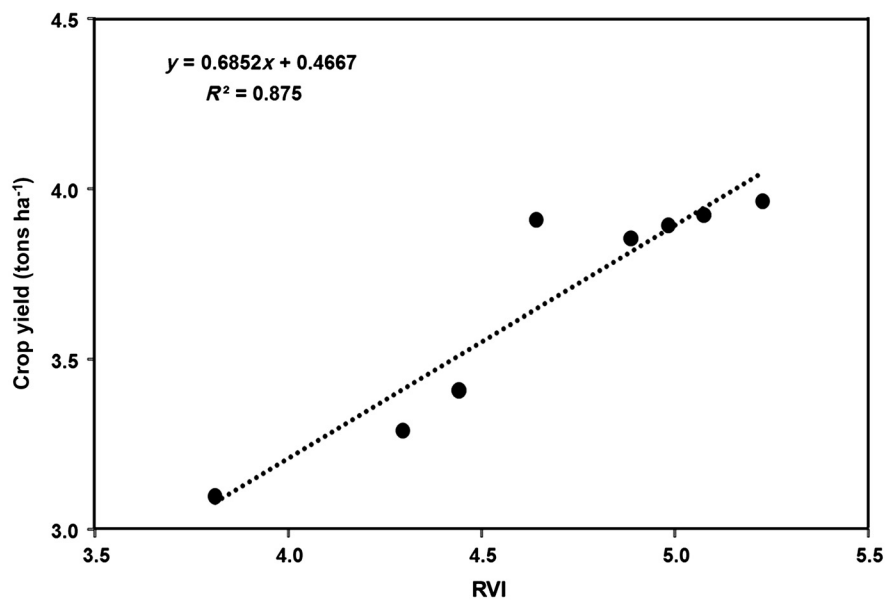


Fig. 8 Relationship between average ratio vegetation index (RVI) of the rice crop in Larkana district and the average crop yield from 2006 to 2013. RVI is determined from temporal imagery of the area captured 60 to 70 days after sowing of crop.

$$\text{Crop yield} = 0.6852 \text{ RVI} + 0.4667. \quad (10)$$

3.4 Accuracy Assessment of Rice Area Model

Correlation of the area under rice cultivation reported by CRS in Larkana district from 2006 to 2013 and estimated from the model [Eq. (8)] was assessed with the three statistical parameters ME, MBE, and RMSE. The results show a strong relationship between reported and estimated area, with ME = 0.984, MBE = -20,304 ha, and RMSE = 20,560 ha, given in Figure 9. The MBE statistics revealed that the area model underestimates the area under rice cultivation in the district.

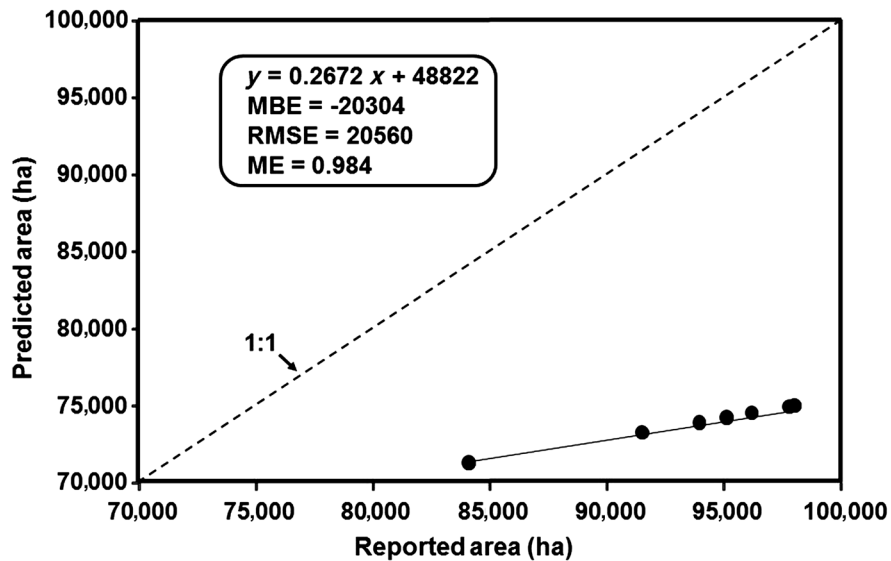


Fig. 9 Correlation of reported and predicted rice area of Larkana district, Sindh, Pakistan.

4 Discussion

In this study, we analyzed the use of Landsat 7 ETM+ satellite imagery for estimation and monitoring of rice crop yield and production. The remote sensing methodology was trained and calibrated against yield and production numbers reported by the Government of Sindh Crop Reporting Service. Based on the statistical parameters MBE, RMSE, and ME and a visual inspection of the agreement between the area reported by CRS and the remote sensing-derived area, we conclude that the remote sensing-derived rice-cropped area can be predicted from Landsat ETM+ data if adjusted to compensate for area underestimation. This can be accomplished using a regression estimator to adjust estimated to reported area. Regression estimator adjustment for remote sensing-derived area estimates is a commonly used technique.^{40,41} In this study, we used eight data points for deriving a regression equation relating Landsat-derived area to the CRS-reported area. From a statistical point of view, this limited number of points is typically not considered enough for deriving a regression model, and is a potential limitation of the described approach. However, using a limited number of data points under these circumstances is not uncommon.

The satellite imagery was not atmospherically corrected, as it is unnecessary for the image classification method used in the study. Due to cloud cover, satellite imagery was not acquired on the same date for different years. Because there is a 10- to 15-day variation in the sowing of crops in Larkana district, 5 to 15 days difference in acquisition of images is unlikely to impact the results of study.

Images from the Landsat 7 ETM+ sensor are compromised by stripes of missing data resulting from the failed SLC. The stripes are also apparent in our study area. However, the effect is small, because the study area falls close to the center of the scene and the proportion of missing data is only 3% to 5%. In this analysis, we compensate for the missing data by assuming that the proportion of rice versus nonrice is the same within the small areas that are missing as it is in the remainder of the district. This shortcoming does not invalidate the methodology; it is rather a deficiency of the input data and can easily be addressed in future studies by using imagery from Landsat 8 and the Sentinel-2 satellites.

The satellite-based monitoring of rice and other crops is of prime importance in Pakistan as well as in countries with rice cultivation and has a number of advantages compared to assessments solely based on ground data collection. The Landsat satellite allows wall-to-wall coverage of the province and includes hard-to-access areas. It is independent of challenges associated with the use of ground-based crop reporters, including human error in field data collection and data entry, delays in getting the data from the field to the office, logistical complications in data collection, and delivery due to natural disasters, in particular flooding and other reasons. At

the same time, the satellite-derived estimates also have drawbacks. This includes the underestimation of area as discussed earlier, the dependence on cloud-free imagery, which might not be available for all years, and the need for remote sensing data processing and analysis by a trained specialist. Satellite-based monitoring still requires field data and long-term, independently derived yield and production statistics for algorithm training and calibration. It is not meant to replace, but rather complement existing systems for the production of statistical crop estimates. The main value of the new methodology comes from more timely estimates much earlier in the growing season than what is possible with the existing ground-based system, and to provide reliable data in cases where previous systems have failed or reacted with long-delayed responses such as in the case of natural disasters or administrative challenges with managing and supporting large numbers of crop reporters stationed in the field.

5 Conclusions

This study investigates the use of Landsat imagery time series for rice yield and production estimates for Pakistan using the study area in Larkana district in Sindh province as a test case. A high correlation was observed between remote sensing-derived and reported area; however, the first systematically underestimated the latter. High correlations were also observed between peak NDVI and reported rice yield for the years 2006 to 2013. RVI performed slightly worse. These results show great promise for the use of remote sensing data for more timely and efficient rice yield and production estimates, which can be calculated several months before the official, field-based numbers are released by the provincial government. For this study, only a few years of data were available for training and calibrating the remote sensing time series analysis. This work will continue as more data become available. The overall importance of crop monitoring in general and of more efficient satellite-based monitoring in particular is increasing every year with the advent of severe climate change impacts expected over the coming decades and with the increasing frequency of major floods, which are thought to be related to climate change effects already. The importance of large-scale agricultural monitoring is also increasing due to increasing pressure on land and water resources resulting from a quickly growing population and from the challenge of inadequately maintained and static or contracting irrigation systems, which are the lifeline for agricultural activities in the very arid climate of southern Pakistan.

Acknowledgments

We thank the Norman E. Borlaug International Agricultural Science and Technology Fellowship Program for providing eight weeks of training fellowship to Altaf Ali Siyal to undertake two months training at the Department of Geography, University of Maryland. The Sindh Agriculture University, Tandojam, Pakistan is also highly acknowledged for granting ex-Pakistan leave to Dr. Siyal.

References

1. IRRI, *IRRI Rice Almanac 1993–1995*, p. 125, International Rice Research Institute, Manila (1993).
2. G. S. Khush, “What it will take to feed 5 billion rice consumers in 2030” *Plant Mol. Biol.* **59**, 1–6 (2005).
3. FAO, “Rice market monitor. Trade and markets division,” *F. A. O. U. N.* **XV**(4), 1–2 (2012).
4. C. M. Yang, C. C. Liu, and Y. W. Wang, “Using FORMOSAT-2 satellite data to estimate leaf area index of rice crop,” *J. Photogram. Remote Sens.* **13**, 253–260 (2008).
5. USDA, “World agricultural production. Foreign agricultural service,” <http://www.fas.usda.gov/psdonline/psdreport.aspx?hidReportRetrievalName=BVS&hidReportRetrievalID=893&hidReportRetrievalTemplateID=1> (2013).
6. N. A. Memon, “Rice: important cash crop of Pakistan,” *Pak. Food J.*, pp. 21–23, 2013 <http://www.foodjournal.pk/Sept-Oct-2013/Sept-Oct-2013-PDF/Exclusive-article-Rice.pdf> (14 October 2014).

7. Dawn, "Pakistan rice production up," *Daily Dawn*, 2012, <http://dawn.com/news/765616/pakistan-rice-production-up> (02 September 2014).
8. J. F. Huang et al., "Rice yield estimation using remote sensing and simulation," *JZUS* **3**, 461–466 (2002).
9. X. T. S. Xiao et al., "Mapping paddy rice agriculture in southern China using multi-temporal MODIS images," *Remote Sens. Environ.* **95**, 480–492 (2005).
10. M. Reynolds et al., "Estimation crop yields and production by integrating the FAO crop specific water balance model with real-time satellite data and ground-based ancillary data," *Int. J. Remote Sens.* **21**(18), 3487–3508 (2000).
11. I. W. Nuarsa et al., "Spectral characterization of rice field using multi-temporal landsat ETM+ data," *Int. J. Remote Sens. Earth Sci.* **2**, 65–71 (2005).
12. X. Pan et al., "Remote sensing of phytoplankton pigment distribution in the United States northeast coast," *Remote Sens. Environ.* **114**, 2403–2416 (2010).
13. I.W. Nuarsa, F. Nishio, and C. Hongo, "Rice yield estimation using Landsat ETM+ Data and field observation," *J. Agri. Sci.* **4**(3), 45–56 (2011).
14. M. S. Rasmussen, "Operational yield forecast using AVHRR NDVI data: reduction of environmental and inter-annual variability," *Int. J. Remote Sens.* **18**, 1059–1077 (1997).
15. C. Huang et al., "Derivation of a tasseled cap transformation based on Landsat 7 at-satellite reflectance," *Int. J. Remote Sens.* **23**, 1741–1748 (2002).
16. M. S. Mkhabela et al., "Crop yield forecasting on the Canadian Prairies using MODIS NDVI data," *Agric. For. Meteorol.* **151**, 385–393 (2011).
17. J. Dempewolf et al., "Performance of vegetation indices for wheat yield forecasting for Punjab, Pakistan," in *American Geophysical Union, Fall Meeting*, Abstract #B41A-0388 (2013).
18. J. Dempewolf et al., "Wheat yield forecasting for Punjab Province from vegetation index time series and historic crop statistics," *Remote Sens.* **6**, 9653–9675 (2014).
19. S. Peng et al., "Grain yield of rice cultivars and lines developed in the Philippines since 1966," *Crop Sci.* **40**, 307–314 (2000).
20. W. G. M. Bastiaanssen and S. Ali, "A new crop yield forecasting model based on satellite measurements applied across the Indus Basin, Pakistan," *Agric. Ecosyst. Environ.* **94**, 321–340 (2003).
21. A. J. Richardson et al., "Remotely-sensed spectral indicators of sorghum development and their use in growth," *Agri. Meteorol.* **26**, 11–23 (1982).
22. S. Goward et al., "Historical record of Landsat global coverage: Mission operations, NSLRSDA, and international cooperator stations," *Photogramm. Eng. Remote Sens.* **72**, 1155–1169 (2006).
23. J. G. Masek et al., "North American forest disturbance mapped from a decadal Landsat record," *Remote Sens. Environ.* **112**, 2914–2926 (2008).
24. M. A. Wulder et al., "Landsat continuity: Issues and opportunities for land cover monitoring," *Remote Sens. Environ.* **112**, 955–969 (2008).
25. <http://glovis.usgs.gov>
26. D. Johnson and R. Mueller, "The 2009 cropland data layer," *Photogramm. Eng. Remote Sens.* **76**(11), 1201–1205 (2010).
27. G. Chander, B. L. Markham, and D. L. Helder, "Summary of current radiometric calibration coefficients for Landsat MSS, TM, ETM+, and EO-1 ALI sensors," *Remote Sens. Environ.* **113** (5), 893–903 (2009).
28. L. Breiman et al., "Classification and regression trees, Wadsworth International Group, Monterey, California (1984).
29. M. C. Hansen et al., "Global land cover classification at 1 km spatial resolution using a classification tree approach," *Int. J. Remote Sens.* **21**, 1331–1364 (2010).
30. P. Potapov et al., "Quantifying forest cover loss in Democratic Republic of the Congo, 2000–2010, with Landsat ETM+ data," *Remote Sens. Environ.* **122**, 106–116 (2012).
31. J. Storey, P. Scaramuzza, and G. Schmidt, "Landsat 7 scan line corrector-off gap-filled product development" in *Proc. Pecora 16 'Global Priorities in Land Remote Sensing'*, Sioux Falls, South Dakota, pp. 23–27 (2005).

32. S. M. Ali and M. J. Mohammed, "Gap-filling restoration methods for ETM+ sensor images," *Iraqi J. Sci.* **54**(1), 206–214 (2013).
33. J. W. Rouse et al., "Monitoring vegetation systems in the Great Plains with ERTS," in *Proc. Third ERTS-1 Symp.*, NASA Goddard, NASA SP-351, pp. 309–317 (1974).
34. <http://pekko.geog.umd.edu/glam/pakistan/zoom2.php>
35. G. S. Birth and G. Mcvey, "Measuring the color of growing turf with a reflectance spectrophotometer," *Agron. J.* **60**, 640–643 (1968).
36. C. J. Willmott, "Some comments on the evaluation of model performance," *Bull. Am. Meteorol. Soc.* **63**(11), 1309–1313 (1982).
37. A. K. Singh et al., "Validation of CropSyst simulation model for direct seeded rice-wheat cropping system," *Curr. Sci.* **104**(10), 1324–1331 (2013).
38. B. D. Wardlow and L. E. Egbert, "State-level crop mapping in the US Central Great Plains agro-ecosystem using MODIS 250-meter NDVI data," in *Pecora 16 Symp.*, pp. 25–27 (2005).
39. R. D. Jackson and A. R. Huete, "Interpreting vegetation indices," *Prevent. Veterinary Med.* **11**, 185–200 (1991).
40. Y. Oguro et al., "Monitoring of rice field by Landsat-7 ETM+ and Landsat-5 TM Data," presented at *22nd Asian Conf. on Remote Sensing*, pp. 5–9, Singapore (2001).
41. E. Carfagna and F. J. Gallego, "Using remote sensing for agricultural statistics" *Int. Stat. Rev.* **73**(3), 389–404 (2005).

Altaf Ali Siyal received his ME degree in irrigation and drainage from Sindh Agriculture University, Tandojam, Pakistan, in 1998. He received his PhD from Cranfield University, United Kingdom, in 2001. He did his postdoctorate research at USDA-ARS Salinity Lab, Riverside California, and CSIRO, Townsville, Australia. Currently, he is working as a professor and chairman at Sindh Agriculture University, Tandojam, Pakistan.

Jan Dempewolf received his PhD in geography from the University of Maryland (UMD) in 2007 and his diploma (Master of Science) in geoecology from the University of Bayreuth, Germany. He is an assistant research professor at UMD and has expertise in agriculture, forest and natural resource monitoring using remote sensing, and GIS tools.

Inbal Becker-Reshef received her PhD in 2012 from the Department of Geographical Sciences at UMD. She is a codirector of the Center for Global Agricultural Monitoring Research and an associate research professor at UMD. Her work is focused on crop monitoring at national to global scales using remote sensing and GIS, with an emphasis on transitioning viable remote sensing-based methods into operational monitoring systems.